Fenton Chemistry and Iron Chelation under Physiologically Relevant Conditions: Electrochemistry and Kinetics

ARTICLE *in* CHEMICAL RESEARCH IN TOXICOLOGY · NOVEMBER 2006

Impact Factor: 3.53 · DOI: 10.1021/tx060101w · Source: PubMed

5 AUTHORS, INCLUDING:

Reinhard Kissner
ETH Zurich
69 PUBLICATIONS **2,119** CITATIONS
SEE PROFILE

Willem H Koppenol
ETH Zurich
223 PUBLICATIONS **13,565** CITATIONS
SEE PROFILE

Articles

Fenton Chemistry and Iron Chelation under Physiologically Relevant Conditions: Electrochemistry and Kinetics

Martin Merkofer,[†] Reinhard Kissner,[†] Robert C. Hider,[‡] Ulf T. Brunk,[§] and Willem H. Koppenol*[,†]

Laboratorium für Anorganische Chemie, Departement Chemie und Angewandte Biowissenschaften, ETH Zürich, CH-8093 Zürich, Switzerland, Department of Pharmacy, King's College London, Franklin-Wilkins Building, 150 Stamford Street, London SE1 9NN, United Kingdom, and Department of Pharmacology, University of Linköping, SE-581 85 Linköping, Sweden

Received May 10, 2006

The goal of iron-chelation therapy is to reduce the levels of labile plasma iron, and intravenously administered desferrioxamine is the gold standard of therapeutic agents. Hydroxypyridinones, e.g., CP20 (3-hydroxy-1,2-dimethylpyridin-4(1*H*)-one), are used or are under investigation as orally administered iron chelators. We determined electrode potentials of CP20, the related hydoxypyridones CP361, CP363, and CP502, and ICL670 (4-[3,5-bis(2-hydroxyphenyl)-1*H*-1,2,4-triazol-1-yl]benzoic acid) under physiologically relevant conditions to address the question of whether iron in the presence of these chelating agents can carry out Fenton chemistry in vivo. We found that iron(III) but not iron(II) binds tightly to both CP20 and ICL670 at pH 7 and higher, compared to nearly complete binding of 1 μM iron(II) to 10 μM desferrioxamine at pH 7.4 The electrode potentials of the hydroxypyridinones shift to more negative values with decreasing pK_a values at lower concentrations of iron(III) (0.02 mM) and ligand (0.1 mM). The electrode potential of the iron−CP20 system decreases as a function of increasing pH, with a minimum near pH 10.5. We estimate an electrode potential for the ascorbyl radical/ascorbate couple under physiological conditions of +105 mV, which is higher than the electrode potential of the iron(III) complex of CP20 at all concentrations of iron. The rate of oxidation of iron(II) in the presence of CP20 by hydrogen peroxide increases with the concentrations of both ligand and peroxide. Although iron(II) is oxidized by hydrogen peroxide, the thus-formed $Fe^{III}(CP20)_3$ complex cannot be reduced by ascorbate. Therefore, the tight binding of iron(III) by this class of chelators prevents redox cycling.

Introduction

The toxicity caused by excessive amounts of iron in iron-overload diseases is probably mediated through the catalytic generation of oxy radicals (*1*). Chronic iron overload arises in several clinical conditions, for example, after blood transfusions for the treatment of certain anemias, including thalassemia (*2*, *3*). Since transferrin, an iron-transport protein, is present in excess in healthy individuals, there should be, in principle, no "free" iron present in plasma, but the iron in plasma that causes harmful reactions is the form not bound to iron proteins, which include ferritin and hemoglobin as well as transferrin. The chemical nature of this non-transferrin-bound iron (NTBI)[1] is unclear at the present time. It has been proposed that NTBI in plasma is stabilized by coordination to both citrate and albumin (*4*). Cabantchik et al. (*5*) named the chelatable and redox-active part of NTBI "labile plasma iron" (LPI). The fraction of NTBI present as LPI depends on the degree of iron overload: in hemochromatosis, the fraction ranges from 0 to 80%, and, in thalassemia patients, it may be even higher. The values for NTBI fall in the range 1−10 μM in patients that suffer from iron overload (*5*−*7*). The goal of iron-chelation therapy is to reduce the levels of LPI, preferably by means of orally administered iron chelators, but the gold standard of therapeutic agents has been desferrioxamine, which is administered intravenously.

Transition-metal complexes participate in redox cycling only when two conditions are met, namely, that the oxidized complex can be reduced and that the reduced complex can transfer an electron to a peroxide (*8*, *9*). In the case of hydrogen peroxide and ascorbate, this implies that metal complexes with standard electrode potentials larger than +0.39 V ($H_2O_2/HO^\bullet$, H_2O, pH 7) or smaller than +0.28 V (ascorbyl/monohydroascorbate, pH 7) (*10*) cannot catalyze the set of reactions defined by eqs 1 and 2, where X indicates ligands bound to iron.

$$Fe^{2+}X + H_2O_2 + H^+ \rightarrow Fe^{3+}X + H_2O + HO^\bullet \quad \text{(Fenton reaction)} \quad (1)$$

$$Fe^{3+}X + HAsc^- \rightarrow Fe^{2+}X + H^+ + Asc^{\bullet-} \quad (2)$$

* To whom correspondence should be addressed. Fax: 41 44 632 1090. E-mail: koppenol@inorg.chem.ethz.ch.

[†] ETH Zürich.

[‡] King's College London.

[§] University of Linköping.

[1] Abbreviations: GSH, glutathione; LPI, labile plasma iron; NTBI, non-transferrin-bound iron; CP20, 3-hydroxy-1,2-dimethylpyridin-4(1*H*)-one; CP361, 3-hydroxy-2-(1-hydroxyethyl)-1,6-dimethylpyridin-4(1*H*)-one; CP363, 3-hydroxy-2-(1-methoxyethyl)-1,6-dimethylpyridin-4(1*H*)-one; CP502, 3-hydroxy-*N*,1,6-trimethyl-4-oxo-1,4-dihydropyridine-2-carboxamide; CP509, 3-hydroxy-*N*,*N*,1,6-tetramethyl-4-oxo-1,4-dihydropyridine-2-carboxamide; ICL670, 4-[3,5-bis(2-hydroxyphenyl)-1*H*-1,2,4-triazol-1-yl]benzoic acid; superoxide, dioxide(1•−).

10.1021/tx060101w CCC: $33.50
Published on Web 09/27/2006

Chart 1. Structures of the Oral Iron Chelators

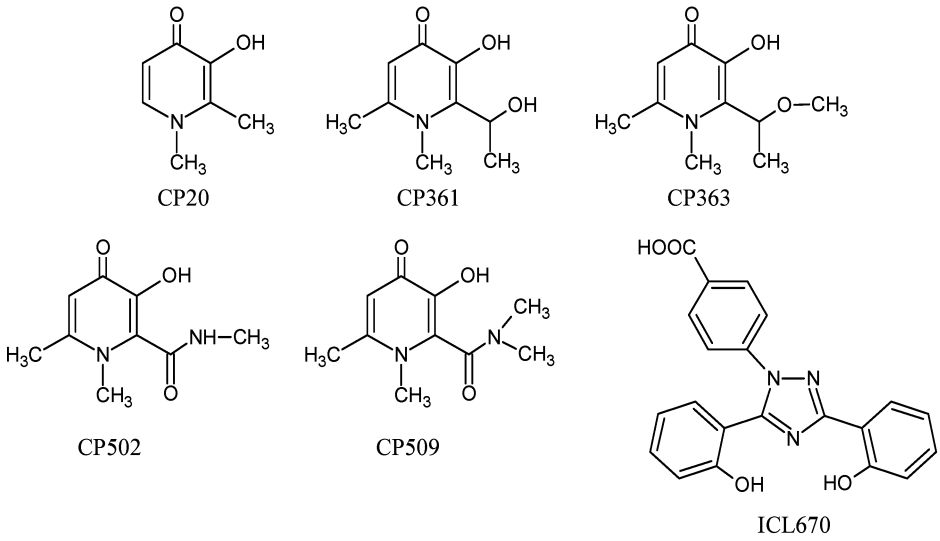

The electrode potential of the hydrogen peroxide/water, hydroxyl radical couple was first reported as +0.80 V (*11*) and later as +0.32 V (*12*). On the basis of the Gibbs energy of formation of hydrogen peroxide (*13*) and the electrode potential of the hydroxyl radical/water couple (*14*), we now propose a value of +0.39 V at pH 7. However, these values refer to standard conditions, which do not apply in biological systems.

Recently, we determined the redox properties of the iron complexes of the oral iron chelators CP20, CP502, CP509, and ICL670 (Chart 1) and concluded that the electrode potentials are dependent on pH and the concentrations of iron and ligand (*15*). In an earlier paper, we presented pulse radiolysis evidence that the reason for the positive shift of the electrode potential is incomplete formation of the iron(II) complex (*16*). In the present work, we determine rate constants for the reactions of iron(II)−hydroxypyridinone complexes with hydrogen peroxide and provide additional electrochemical data for the iron complexes of CP20, CP361, CP363, CP502, and ICL670. In the past, standard electrode potentials have been invoked in discussions of whether iron bound to such chelating agents redox-cycle or not. However, physiologically relevant conditions are far removed from the standard condition; thus, it is necessary to estimate the magnitude of electrode potentials under conditions present in vivo, i.e., micromolar concentrations of iron and chelator near pH 7. These potentials then should be compared with those of possible reductants, such as monohydrogen ascorbate, and oxidants, such as hydrogen peroxide, also estimated for physiologically relevant conditions. Our estimates of these nonstandard electrode potentials indicate that the iron chelates listed above do not participate in redox-cycling in vivo.

Materials and Methods

Materials. All chemicals used were of analytical reagent grade. CP361, CP363, and CP502 were synthesized and characterized as reported by Liu et al. (*17, 18*). $Fe(NO_3)_3 \cdot 9H_2O$ and $FeSO_4 \cdot 7H_2O$ were used to prepare the iron(III) and iron(II) complexes, respectively. Hydrogen peroxide stock solutions were prepared from Merck analyzed reagent 30% hydrogen peroxide. Water was purified by a Millipore Milli-Q unit fed with deionized water.

Instruments and Methods. Stopped-flow experiments were carried out at 25 °C and ambient pressure with an Applied Photophysics SX 17MV, or with an Applied Photophysics SX 18MV stopped-flow spectrophotometer (Leatherhead, Surrey, Great Britain). A standard solution of 0.10 M hydrogen peroxide in 0.1 M Tris buffer at pH 7.2 was diluted with Tris buffer of the same concentration and pH in a 50 mL Schlenk vessel and purged for 30 min with argon. Solutions of CP20 in 0.1 M Tris buffer, pH 7.2, were evacuated and saturated with argon at least five times before the appropriate amount of iron(II) was added. Both solutions were handled in gastight syringes. The pH was 7.2 after mixing in the stopped-flow spectrophotometer. Formation of the Fe^{III}(CP20) complex was followed at 450 nm.

Electrochemical measurements were performed with an AMEL 2049 potentiostat and an AMEL 568 function generator as described before (*15*). Potentials were measured against a Ag/AgCl (3 M KCl) reference electrode (+0.200 V vs normal hydrogen electrode, NHE). All discussions of potentials in the text are for values vs the NHE. Potential scales of voltammograms are based on the experimentally used Ag/AgCl system.

Species distribution diagrams were calculated with the SPEC program (R. Kissner, ETHZ). In this program, which was designed to calculate the species distribution in solution from known formation constants and total concentrations, the Newton−Raphson algorithm is applied to solve the system of nonlinear partition equations by the tangential method.

Results

Iron Distribution Curves. We plotted speciation diagrams (Figure 1) for the iron(III) and iron(II) complexes of ICL670 (Figure 1A) and CP20 (Figure 1B) at pM conditions: $[Fe^{2+}] = [Fe^{3+}] = 0.5\ \mu M$, [ligand] = 10 μM, pH 7.4. We assumed that the ratios β_3:β_2 and β_3:β_1 for iron(II) are similar to those of iron(III), as the binding constants β_1 and β_2 for iron(II) are not known. The data for Figure 1 were generated from data in Tables 1 and 2. While iron(III) binds tightly to both CP20 and ICL670 at pH 7 and higher, iron(II) does not. The amount of iron(II) bound to desferrioxamine, a well-studied ligand, at pH 7.4 and the same concentrations of iron and ligand is 96.5%. This percentage is based on the stability constant of the complex of desferrioxamine with iron(II), which is calculated from the standard electrode potential of the iron(III)/iron(II) couple, that of the iron(III)/iron(II)−desferrioxamine couple, and the stability constant of the complex of iron(III) with desferrioxamine. Hence, the tendency to dissociate follows the order hexadentate < tridentate < bidentate, as expected.

Influence of the pK_a Value on the Electrode Potential. Figure 2 shows cyclic voltammograms of the iron complexes of CP502, CP20, CP361, and CP363 in Tris buffer at pH 7.2. With the exception of CP502, at lower concentrations, i.e., 0.02 mM iron(III) and 0.1 mM ligand, the electrode potential shifts

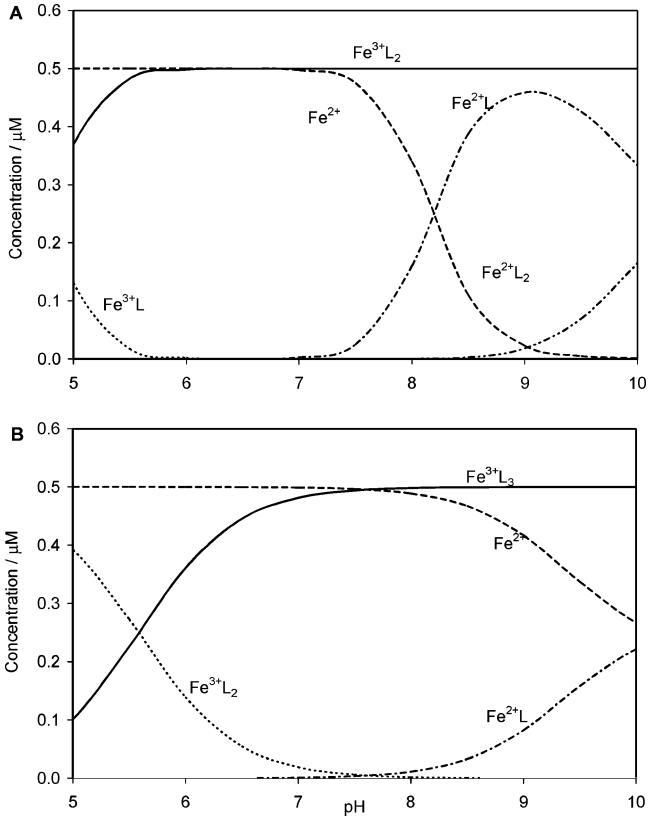

Figure 1. Iron speciation in the presence of iron chelators ([Fe^{2+}] = [Fe^{3+}] = 0.5 μM): (A) [ICL670] = 10 μM, $Fe^{3+}L_2$ (—), $Fe^{3+}L$ (•••), $Fe^{2+}L_2$ (••-••), $Fe^{2+}L$ (•-•), Fe^{2+} (---); (B) [CP20] = 10 μM, $Fe^{3+}L_3$ (—), $Fe^{3+}L_2$ (•••), $Fe^{2+}L$ (•-•), Fe^{2+} (---).

Table 1. pK_a Values and Stability Constants for Iron(III) Complexes

ligand	p$K_{a,1}$	p$K_{a,2}$	p$K_{a,3}$	log K_1	log β_2	log β_3	ref
CP20	3.62	9.76		15.14	26.68	35.92	40
CP361	3.55	8.97				35.5	41
CP502	2.77	8.44				34.3	41
ICL670	3.7	8.80	10.61	22.0	36.9		*23*, *42*
catechol	9.3	~13.3		20.4	35.5	44.9	40
enterobactin	9.2[a]	12.1[a]	12.1[a]	~52[a]			40
transferrin				20.2	33.9		40
desferrioxamine	8.32	8.96	9.55	30.99			40

[a] Estimated.

Table 2. Electrode Potentials (vs NHE) and Stability Constants of Iron(II) Complexes

ligand	pH	temp (°C)	$E°$ (mV)	log β_3	ref
CP20	11	25	−620	12.4	15
CP361	11	25	−610	12.1	this work
CP363	11	25	−558	not determined	this work
CP502	11	25	−535	12.2	15
CP509	11	25	−535	not determined	15
ICL670	11	25	−600	not determined[a]	*23*, *42*

[a] log β_2 = 13.7, log K_1 = 11.5.

to more negative values with decreasing p$K_{a,2}$ values of the hydroxypyridinone (Figure 2A). Although the p$K_{a,2}$ of CP502 is the lowest in the series, its electrode potential shifts to positive values, because the soft nitrogen atom in the amide group stabilizes the iron(II) ion (*15*). At higher concentrations of ligand and metal, 0.1 mM iron(III) and 0.5 mM ligand (Figure 2B), the differences between the various metal complexes are not as large. The electrode potential of the iron complex of CP502 could not be measured under these conditions and was estimated as described earlier (*15*). To determine the standard electrode

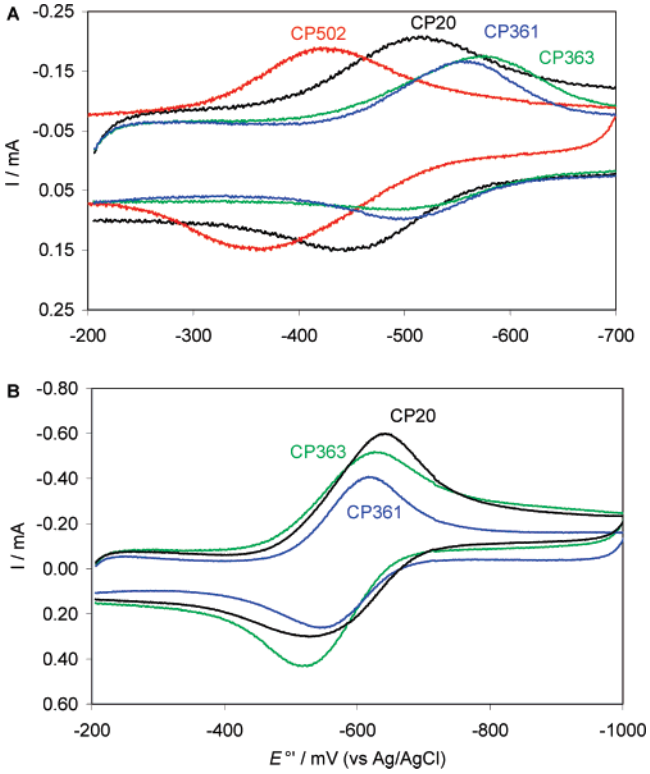

Figure 2. Cyclic voltammograms of iron complexes of oral chelators: (A) $[Fe]_{total}$ = 0.02 mM, $[ligand]_{total}$ = 0.1 mM; (B) $[Fe]_{total}$ = 0.1 mM, $[ligand]_{total}$ = 0.5 mM. Voltammograms recorded with a mercury hanging-drop electrode in 0.1 M Tris buffer at pH 7.2, scan rate 100 mV s^{-1}. Ligands: CP20 (black), CP361 (blue), CP363 (green), and CP502 (red).

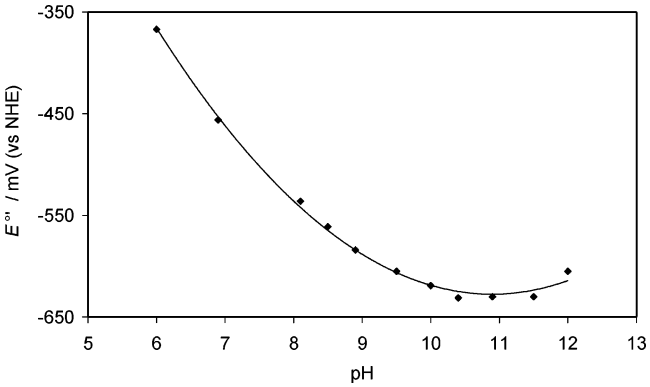

Figure 3. Electrode potential of the $Fe^{III}(CP20)_3/Fe^{II}(CP20)_x$ couple as a function of pH. Electrode potentials determined by cyclic voltammetry, scan rate 100 mV s^{-1}, $[Fe]_{total}$ = 1 mM, and $[CP20]_{total}$ = 5 mM.

potentials, we measured the same complexes with 1 mM iron and 5 mM ligand at pH 11; under these conditions, the electrode potential did not shift to more negative values with increased pH (Table 2).

Figure 3 presents the electrode potential of the iron−CP20 system as a function of pH, as obtained by cyclic voltammetry. The electrode potential decreases until the pH reaches a value of 10.5 and then remains constant. At pH 12, the potential increases again, consistent with the formation of iron−hydroxo species.

Electrode Potentials of the Ascorbyl/Monohydroascorbate and Hydrogen Peroxide/Hydroxyl, Water Couples under Physiologically Relevant Conditions. Comparison with That of the Iron(III)/Iron(II)−CP20 Complex. To determine whether the iron(III) complexes of CP20, CP502, CP361,

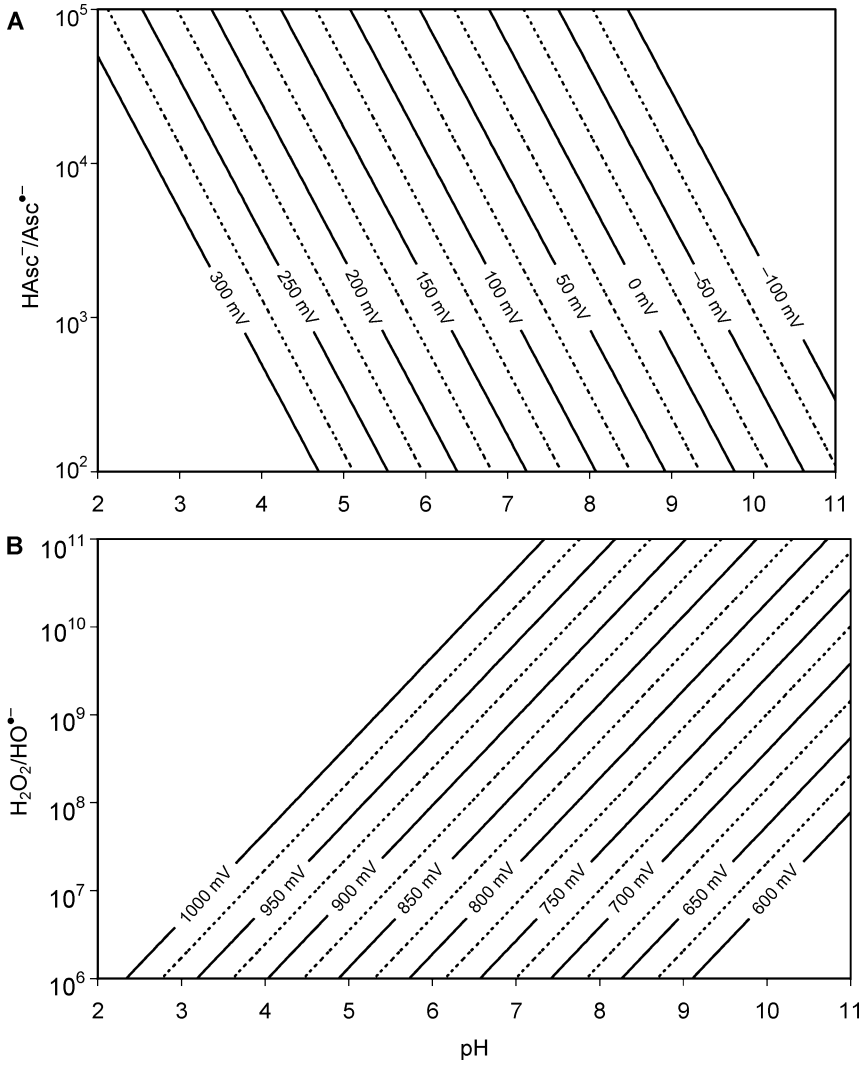

Figure 4. Electrode potentials as a function of pH and concentration at biological conditions: (A) $Asc^{\bullet -}$/$HAsc^-$ couple, (B) $H_2O_2/OH^{\bullet}$, H_2O couple.

CP363, and ICL670 are able to redox-cycle under physiologically relevant conditions, we compared the electrode potentials of these complexes with the one-electron electrode potentials of the ascorbyl/monohydroascorbate and the hydrogen peroxide/water, hydroxyl radical couples under physiological conditions.

The pH-dependent electrode potential of the ascorbyl/monohydroascorbate couple at pH 7 is +0.282 V (*10*), and that of the hydrogen peroxide/water, hydroxyl radical couple is +0.39 mV. Figure 4 shows the pH and concentration dependence of the electrode potentials of these couples estimated under biologically relevant conditions. On the basis of the assumption that the steady-state concentrations of the ascorbyl radical and ascorbate in a cell are 10^{-6} and 10^{-3} M, respectively (*19*), then the physiological electrode potential is ca. +105 mV.

El-Jammal and Templeton (*20*) derived a formula to calculate electrode potentials of iron−hydroxypyridinone complexes that includes pH, the ligand:metal ratio, the $pK_{a,2}$ value of the hydroxypyridinone, and the β_3 stability constant. We used this formula to calculate the electrode potentials of the iron−CP20 complex at micromolar concentrations to obtain values that are representative for physiological conditions. In Figure 5, we compare calculated and experimentally determined values of the electrode potentials for the iron−CP20 complex in the ascorbyl/monohydroascorbate system. By cyclic voltammetry, we could measure electrode potentials only at iron concentrations higher than 20 μM. The experimental findings demonstrate that ascorbate does not reduce CP20-complexed iron(III) under these conditions.

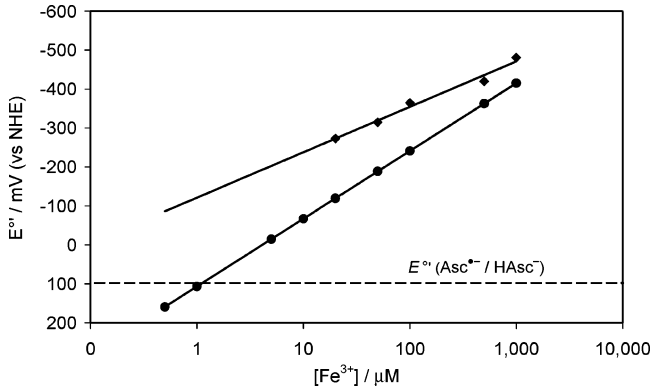

Figure 5. Electrode potential of CP20 as a function of iron concentration at pH 7.2 and ligand:metal = 5:1: (◆) experimentally determined values, (●) values calculated with the formula derived by El-Jammal and Templeton (*20*). The electrode potential of $Asc^{\bullet -}$, $H^+/HAsc^-$ under physiological conditions (+105 mV) was calculated in this work.

Kinetics of the Reaction of the Fe^{II}(CP20) Complex with Hydrogen Peroxide. At a given iron concentration, the rate of reaction with hydrogen peroxide is positively dependent on the CP20 concentration (Figure 6). The rate constants for the

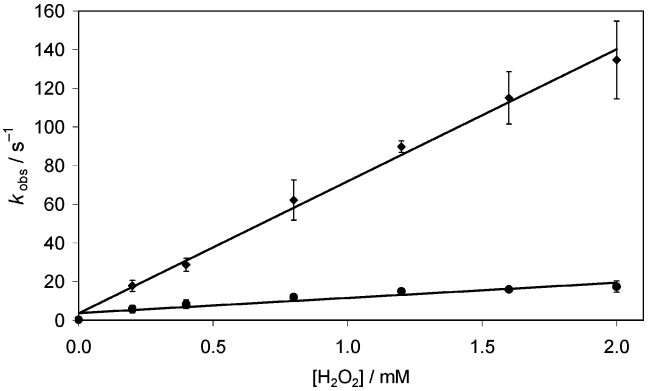

Figure 6. Observed rate constant for the reaction of iron(II)−CP20 with hydrogen peroxide as a function of hydrogen peroxide concentration at pH 7.2 and 25 °C, [Fe^{2+}] = 20 μM, [CP20] = 100 μM (◆) and 40 μM (●).

reaction of iron(II) with excess hydrogen peroxide at 25 °C and pH 7.2 are (6.8 ± 0.2) × 10^4 and (8 ± 1) × 10^3 M^{-1} s^{-1} in the presence of 5-fold and 2-fold excess CP20, respectively (20 μM iron(II), 100 or 40 μM ligand). At higher pH, the reaction becomes faster (data not shown). The rate constant for the reaction of hydrogen peroxide with the Fe^{II}(CP502) complex is (6.1 ± 0.5) × 10^4 M^{-1} s^{-1} at pH 7.2, 20 μM iron(II), 100 μM ligand, and 25 °C (data not shown). Thus, the reaction rate constants under those conditions are similar for both hydroxypyridinone ligands CP20 and CP502. Had accessibility of iron(II) to hydrogen peroxide been a factor, we would have expected the rate of the reaction to *decrease* with increasing ligand concentration. Moreover, because the majority of iron(II) ions are coordinated to only one CP20 molecule (see Figure 1 of ref *16*) and labile water or form Tris buffer complexes of unknown stochiometry, we assume that thermodynamic stabilization of the iron(III) product is the source of the increase in rate: at a 5:1 ratio of ligand to iron(III), the complex $Fe^{III}(CP20)_3$ will be formed completely (*16*), but not at a ratio of 2:1. The hydroxyl radicals produced by the Fenton reaction react with Tris buffer (*21*), which is present in excess over iron and CP20. The generalized reaction equation related to the above rate constants is

$$Fe^{II}L, Fe^{II}Tris_n + H_2O_2 + mL \rightarrow Fe^{III}L_3 + OH^- + {}^{\bullet}OH \quad (3)$$

with $n = 0-6$ and $m = 2-3$. The corresponding rate law could be written as

$$d[Fe^{III}L_3]/dt = k[H_2O_2][Fe(II)]_{tot} \quad (4)$$

Reaction of Hydrogen Peroxide with the $Fe^{III}(CP20)_2$ Complex. Nishida et al. (*22*) reported that, when peroxide ions and phenol groups are coordinated to the same iron(III) center, the peroxide causes oxidative degradation of the phenol. If CP20 were vulnerable to such degradation, its usefulness as an iron chelator would be questionable. We mixed 20 μM iron(III) and 40 μM CP20 with 2 mM hydrogen peroxide at pH 7.2 and 25 °C, conditions that leave two coordination sites free to be occupied by hydrogen peroxide, thus maximizing the probability of reaction. We found no indication of any degradation of the iron(III) product over a time course of 1000 s monitored at 450 nm, where the $Fe^{III}(CP20)_3$ complex has its maximal absorption coefficient of 4600 M^{-1} cm^{-1}.

Discussion

Thermodynamics. The speciation diagrams (Figure 1) help illustrate why the increase in the electrode potential upon dilution is more pronounced for $Fe^{III}(CP20)_3$ than for $Fe^{III}(ICL670)_2$. First, there is a shift to more positive values, because, under dilute conditions, the iron(II) complexes are not fully formed. In cyclic voltammetry, equilibrium potentials are measured, and thus, the amount of iron(III) complex reduced during the first half of the cycle should be reoxidized during the second half. If the iron(II) complex dissociates after reduction, as is the case with the ICL670 and hydroxypyridinone complexes described here, then the concentration of the iron(II) complex decreases and, according to the Nernst equation, the electrode potential shifts to values larger than that of the standard electrode potential. Second, under comparably dilute conditions, more $Fe^{II}(ICL670)_2$ will be present than $Fe^{II}(CP20)_3$, and for that reason, the potential of the $Fe^{III}/Fe^{II}(CP20)_3$ couple is more sensitive to dilution.

While we detected a pH-dependent change in the electrode potential of the iron−CP20 system and earlier also in that of the iron−ICL670 system (*15*), Steinhauser et al. (*23*) did not report such a change. They determined the standard electrode potential only at high pH and high iron and ligand concentrations, where also the iron(II) complex is completely formed, which is clearly not the case under physiologically relevant conditions (Figure 1A).

Figure 5 shows a calculated and an experimentally determined electrode potential determined for the iron−CP20 complex as a function of the concentration of $Fe^{III}(CP20)_3$, along with that of the ascorbyl/monohydroascorbate couple. The experimental electrode potentials are lower than the calculated ones because the stability constants of the iron(II) complex that influence the electrode potential were not included in the formula derived by El-Jammal and Templeton (*20*). These stability constants are not known and are very difficult to determine, because the electrode potentials of iron(II) complexes of these ligands are low enough to reduce water (*16*). As described by El-Jammal and Templeton (*20*) and Steinhauser et al. (*23*), electrode potentials shift to higher values if the iron(III) complexes are not fully formed, as we have demonstrated (*15*), and approach levels similar to the electrode potential of the ascorbyl/monohydroascorbate couple. It is, thus, important to maintain ligand concentrations at levels high enough for the iron(III) complexes to be fully formed. In Figure 5, we consider only the experimental line, which shows that there is no reduction of iron under these conditions, since the electrode potential of the iron complex remains lower than that of the ascorbyl/monohydroascorbate couple.

Superoxide, which might also be considered a potential reductant of iron(III) in vivo, can be ruled out on both kinetics and thermodynamics grounds. From a kinetic point of view, superoxide is more likely to encounter and react with the dismutases than with iron(III). From a thermodynamic point of view, the electrode potential of the dioxygen/superoxide couple under physiological conditions, namely, ca. 10 μM dioxygen and 0.1 nm superoxide (*24*), is 0.12 V, quite similar to the physiological ascorbyl/monohydroascorbate value of 0.10 V. Although we have not examined all possible phyiological reductants, it appears unlikely that iron−Tris(CP20) complexes participate in Fenton chemistry or redox cycling under physiologically relevant conditions. The similarity of the standard electrode potentials of related chelates (see Table 2) to that of the iron−CP20 complex means that we can extend this conclusion also to these complexes.

To avoid redox cycling in vivo, it is critical that the iron(III) complex is fully formed and not reducible (*15*). The former depends on the ligand concentration and the latter on the

Table 3. Second-Order Rate Constants for Reactions of $Fe^{II}L$ with Hydrogen Peroxide

ligand L	pH	rate constant ($M^{-1}\,s^{-1}$)	ref
atp	4.5	$\sim 2.4 \times 10^3$	43
atp	7.2	$(6.6 \pm 0.3) \times 10^3$	43
atp	8.9	$\sim 2.6 \times 10^4$	43
adp	7.2	$(1.1 \pm 0.2) \times 10^4$	43
utp	7.2	$(5.2 \pm 0.3) \times 10^3$	43
P_2O_7	7.2	$(1.0 \pm 0.2) \times 10^5$	43
citrate	7.2	$(4.9 \pm 0.3) \times 10^3$	43
edda	7.2	7.8×10^4	44
nta	7.2	3×10^4	44
catalase	7.0	7.9×10^6	45
catalase	7.5	2.0×10^7	46
CP20[a]	7.2	$(6.8 \pm 0.2) \times 10^4$	this work
CP502[a]	7.2	$(6.1 \pm 0.5) \times 10^4$	this work
dtcs	7.4	$(6.9 \pm 0.2) \times 10^4$	47
mgd	7.4	$(3.6 \pm 0.1) \times 10^4$	47

[a] The Fenton reaction was studied with these ligands present, to which Fe(II) was only partially bound; see Figure 1 of ref *16*.

electrode potential. For the hydroxypyridinone ligands, as Figure 3 shows, the electrode potential decreases with increasing pH, then levels off, and remains constant at a pH close to the second pK_a. Under these conditions, iron(II) is also fully complexed and no pH-dependent shift of the electrode potential can be detected. Thus, the magnitude of the second pK_a influences the electrode potential at pH 7 under physiological conditions. Similar observations were also made by Crumbliss et al. (*25*) for iron−desferrioxamine. These results imply that, when the pK_a value of the ligand is lower than the physiological pH, small changes in cellular pH will hardly influence the electrode potential. Thus, the ideal iron chelator with respect to redox cycling should, from a thermodynamics point of view, have a low pK_a value and lack soft nitrogen donor atoms in side chains that could stabilize iron(II) and raise the electrode potential.

Kinetics. The nature of NTBI is unclear at the present time, but it is assumed that a proportion of NTBI could be in an oligomeric form stabilized by the citrate present in plasma at a level of 100−120 μM (*4*). At a metal:ligand ratio of 1:10, the electrode potential of the iron(III)/iron(II) couple of the citrate complexes was determined by cyclic voltammetry to be +230 mV in Tris buffer at pH 7.4 (*26*). Consequently, these iron(citrate)$_x$ complexes do have electrode potentials that allow redox cycling and Fenton chemistry. Calculations show that, in the presence of 20 μM CP20, citrate is displaced, and the $Fe^{III}(CP20)_3$ complex is fully formed. Also, the nature of cellular redox-active iron is not known. Let us use an assumed concentration of redox-active iron in the cell of 5 μM to calculate the rate of hydroxyl radical production in a cell. Chance et al. (*27*) studied the rate of hydrogen peroxide production in isolated perfused rat liver by observing the spectral intermediate of the enzyme catalase and arrived at a value of 49 nmol min^{-1} g^{-1} of liver. Assuming that the density of rat liver is 1 g/cm^3, we estimate a rate of production of hydrogen peroxide of 0.82 μM s^{-1}. In erythrocytes, the catalase concentration is ca. 1.9 μM (*28*). If the level of catalase in liver is similar (*29*) and, given a rate constant for the reaction of hydrogen peroxide with catalase of 3.5×10^7 M^{-1} s^{-1} (*28*), the steady-state concentration of hydrogen peroxide in the liver is ca. 10 nM, which is in agreement with the value of Chance et al. (*30*). The presence of a 5 μM pool of cellular redox-active iron does not change the steady-state concentration of hydrogen peroxide, because [catalase]$k_{\text{catalase+hydrogen peroxide}}$ is 300 times larger than [cellular redox-active iron]k_{Fenton}. For k_{Fenton}, we use a rate constant of 6.8×10^4 M^{-1} s^{-1} (Table 3, Fe^{2+} in the presence of CP20). Thus, any consumption of hydrogen peroxide via the Fenton pathway would be insignificant. On the basis of a steady-state concentration of hydrogen peroxide in the nanomolar range and the same Fenton reaction rate constant of 6.8×10^4 M^{-1} s^{-1}, the hydroxyl radical production is estimated at 4×10^{-9} M s^{-1}. This value is an upper limit, because not all of the cellular redox-active iron is in the iron(II) state, and the rate constant used is high for a Fenton reaction (see Table 3). However, since iron does accumulate in the livers of iron-overload patients, the concentration of redox-active iron in liver cells might be higher than 5 μM. We point out that the reaction of cellular redox-active iron(II) with hydrogen peroxide would proceed very slowly at the low concentrations of iron(II) and hydrogen peroxide in vivo.

Biological Relevance. Given the estimated concentrations of hydrogen peroxide, redox-active iron, and catalase in the cytosol and plasma and the values of the rate constants for the Fenton reaction, this reaction does not appear to be a likely source of damage, even when one considers that the damage initiated by one hydroxyl radical can be propagated through, for instance, cycles of lipid peroxidation. However, it has been shown (*31*) that Jurkat cells exposed to low concentrations of hydrogen peroxide die. The authors of this paper argue that hydrogen peroxide, due to its solubility in organic phases (*32*), crosses membranes into the lysosome, where it participates in Fenton chemistry with redox-active iron in the lysosome, with resulting lysosomal labilization, after which the defenses of the cell are overwhelmed. By normal autophagy, the lysosomal compartment executes the turnover of most long-lived proteins and all cellular organelles, resulting in a continuously ongoing, rather intense degradation of a variety of ferruginous macromolecules, e.g., ferritin and mitochondrial complexes (*33*). Consequently, a major part of redox-active iron in the cell is present inside lysosomes, where the local concentrations can be high, making these organelles very sensitive to oxidative stress (*34*, *35*), and chelation of iron in lysosomes has been shown to protect against cell death (*36*). Because proteins are degraded in lysosomes, it is unlikely that catalase is present. Iron complexed with cysteine in the reduced state (*31*) would be eminently capable of Fenton chemistry, given the low electrode potential and because only two cysteines are bound (*37*), thus allowing hydrogen peroxide to replace bound water molecules. Nonbound cysteines would be oxidized to form thiyl radicals, which, being capable of hydrogen abstraction (*38*, *39*), are not innocuous. Although desferrioxamine still binds iron(II) under the conditions of low pH in the lysosome, bidentate and tridentate ligands such as CP20 and ICL670 are less likely to do so given the data in Figure 1, meaning that iron(II) could be oxidized by dioxygen or hydrogen peroxide. Upon oxidation, however, the Fe^{III}Tris-$(CP20)_3$ complex would be formed, which, given the results shown in Figure 5, cannot be reduced by monohydroascorbate and is, thus, redox-inactive. We conclude that CP20, when present at concentrations sufficient to fully complex all iron(III), efficiently sequesters iron to prevent redox-cycling. These conclusions can be extended to the related hydroxypyridone as well as the ICL670 oral chelators.

Acknowledgment. This work was supported by the ETH Zürich, Swiss National Science Foundation, EU (Grant QLK1-CT-2002-00444), and BBW (Grant 01.0397). We thank Dr. P. L. Bounds for comments and help in the preparation of this paper.

References

(1) Halliwell, B., and Gutteridge, J. M. C. (1990) Role of free radicals and catalytic metal ions in human disease: An overview. *Methods Enzymol. 186*, 1−85.

(2) Liu, Z. D., and Hider, R. C. (2002) Design of iron chelators with therapeutic application. *Coord. Chem. Res. 232*, 151−171.
(3) Liu, Z. D., and Hider, R. C. (2002) Design of clinically useful iron(III)-selective chelators. *Med. Res. Rev. 22*, 26−64.
(4) Hider, R. C. (2002) Nature of nontransferrin-bound iron. *Eur. J. Clin. Invest. 32* (Suppl.), 50−54.
(5) Esposito, B. P., Breuer, W., Sirankapracha, P., Pootrakul, P., Hershko, C., and Cabantchik, Z. I. (2003) Labile plasma iron in iron overload: redox activity and susceptibility to chelation. *Blood 102*, 2670−2677.
(6) Breuer, W., Hershko, C., and Cabantchik, Z. I. (2000) The importance of non-transferrin bound iron in disorders of iron metabolism. *Transfus. Sci. 23*, 185−192.
(7) Cabantchik, Z. I., Breuer, W., Zanninelli, G., and Cianciulli, P. (2005) LPI-labile plasma iron in iron overload. *Best Pract. Res. Clin. Haematol. 18*, 277−287.
(8) Koppenol, W. H. (1997) Chemical reactivity of radicals. In *Chemical Toxicology* (Wallace, K. B., Ed.) pp 3−14, Raven Press, New York.
(9) Crichton, R. (2001) *Inorganic Biochemistry of Iron Metabolism*, John Wiley & Sons, Ltd., Chichester, U.K.
(10) Williams, M. H., and Yandell, J. K. (1982) Outer-sphere electron transfer reactions of ascorbate anions. *Aust. J. Chem. 35*, 1133−1144.
(11) Koppenol, W. H. (1976) Reactions involving singlet oxygen and the superoxide anion. *Nature 262*, 420−421.
(12) Koppenol, W. H. (1994) Chemistry of iron and copper in radical reactions. In *Free Radical Damage and its Control* (Rice-Evans, C. A., and Burdon, R. H., Eds.) pp 3−24, Elsevier Science B.V., Amsterdam.
(13) Kern, M. H. (1954) The polarography and standard potential of the oxygen-hydrogen peroxide couple. *J. Am. Chem. Soc. 76*, 4208−4214.
(14) Schwarz, H. A., and Dodson, R. W. (1984) Equilibrium between hydroxyl radicals and thallium (II) and the oxidation potential of OH(aq). *J. Phys. Chem. 88*, 3643−3647.
(15) Merkofer, M., Kissner, R., and Koppenol, W. H. (2004) Redox properties of the iron complexes of CP20, CP502, CP509 and ICL670. *Helv. Chim. Acta 87*, 3021−3034.
(16) Merkofer, M., Domazou, A. S., Nauser, T., and Koppenol, W. H. (2006) Dissociation of CP20 from iron(II)$(cp20)_3$; A pulse radiolysis study. *Eur. J. Inorg. Chem.* 671−675.
(17) Liu, Z. D., Khodr, H. H., Liu, D. Y., Lu, S. L., and Hider, R. C. (1999) Synthesis, physicochemical characterization, and biological evaluation of 2-(1′-hydroxyalkyl)-3-hydroxypyridin-4-ones: Novel iron chelators with enhanced pFe^{3+} values. *J. Med. Chem. 42*, 4814−4823.
(18) Liu, Z. D., Piyamongkol, S., Liu, D. Y., Khodr, H. H., Lu, S. L., and Hider, R. C. (2001) Synthesis of 2-amido-3-hydroxypyridin-4(1*H*)-ones. *Bioorg. Med. Chem. 9*, 563−573.
(19) Griffiths, H. R., and Lunec, J. (2001) Ascorbic acid in the 21st century—more than a simple antioxidant. *Environ. Toxicol. Pharmacol. 10*, 173−182.
(20) El-Jammal, A., and Templeton, D. M. (1996) Iron-hydroxypyridone redox chemistry: Kinetic and thermodynamic limitations to Fenton activity. *Inorg. Chim. Acta 245*, 199−207.
(21) Hicks, M., and Gebicki, J. M. (1986) Rate constants for reaction of hydroxyl radicals with tris, tricine and hepes buffers. *FEBS Lett. 199*, 92−94.
(22) Ito, S., Ishikawa, Y., Nishino, S., Kobayashi, T., Ohba, S., and Nishida, Y. (1998) Interaction between peroxide ion and phenol group which are coordinated to the same iron(III) ion. *Polyhedron 17*, 4379−4391.
(23) Steinhauser, S., Heinz, U., Bartholomä, M., Weyhermüller, T., Nick, H., and Hegetschweiler, K. (2004) Complex formation of ICL670 and related ligands with Fe(III) and Fe(II). *Eur. J. Inorg. Chem.*, 4177−4192.
(24) Koppenol, W. H., and Bounds, P. L. (1989) Hormesis. *Science 246*, 311.
(25) Spasojevic, I., Armstrong, S. K., Brickman, T. J., and Crumbliss, A. L. (1999) Electrochemical behavior of the Fe(III) complexes of the cyclic hydroxamate siderophores alcaligin and desferrioxamine E. *Inorg. Chem. 38*, 449−454.
(26) Engelmann, D. M., Bobier, R. T., Hiatt, T., and Cheng, I. F. (2003) Variability of the Fenton reaction characteristics of the EDTA, DTPA, and citrate complexes of iron. *BioMetals 16*, 519−527.
(27) Oshino, N., Chance, B., Sies, H., and Bücher, T. (1973) The role of H_2O_2 generation in perfused rat liver and the reaction of catalase Compound I and hydrogen donors. *Arch. Biochem. Biophys. 154*, 117−131.
(28) Chance, B., Greenstein, D. S., and Roughton, F. J. W. (1952) The mechanism of catalase action I. Steady-state analysis. *Arch. Biochem. Biophys.* 301−321.
(29) Halliwell, B., and Gutteridge, J. M. C. (1989) *Free Radicals in Biology and Medicine*, Clarendon Press, Oxford.
(30) Chance, B., Sies, H., and Boveris, A. (1979) Hydroperoxide metabolism in mammalian organs. *Physiol. Rev. 59*, 527−605.
(31) Tenopoulou, M., Doulias, P. T., Barbouti, A., Brunk, U., and Galaris, D. (2005) Role of compartmentalized redox-active iron in hydrogen peroxide-induced DNA damage and apoptosis. *Biochem. J. 387*, 703−710.
(32) Walton, J. H., and Lewis, H. (1916) The partition coefficients of hydrogen peroxide between water and certain organic solvents. *J. Am. Chem. Soc. 38*, 633−638.
(33) Terman, A., and Brunk, U. T. (2005) Autophagy in cardiac myocyte homeostasis, aging and pathology. *Cardiovasc. Res. 68*, 355−365.
(34) Yu, Z. Q., Persson, H. L., Eaton, J. W., and Brunk, U. T. (2003) Intralysosomal iron: A major determinant of oxidant-induced cell death. *Free Radical Biol. Med. 34*, 1243−1252.
(35) Persson, H. L., Yu, Z. Q., Tirosh, O., Eaton, J. W., and Brunk, U. T. (2003) Prevention of oxidant-induced lysosomal cell death by lysosomotropic iron-chelators. *Free Radical Biol. Med. 34*, 1295−1305.
(36) Baird, S. K., Kurz, T., and Brunk, U. T. (2006) Metallothionein protects agains oxidative stress-induced lysosomal destabilisation. *Biochem. J. 394*, 275−283.
(37) Lenz, G. R., and Martell, A. E. (1964) Metal chelates of some sulfur-containing amino acids. *Biochemistry 3*, 745−750.
(38) Nauser, T., and Schöneich, C. (2003) Thiyl radicals abstract hydrogen atoms from the α C-H bonds in model peptides: Absolute rate constants and effect of amino acid structure. *J. Am. Chem. Soc. 125*, 2042−2043.
(39) Nauser, T., Pelling, J., and Schöneich, C. (2004) Thiyl radical reaction with amino acid side chains: Rate constants for hydrogen transfer and relevance for posttranslational protein modification. *Chem. Res. Toxicol. 17*, 1323−1328.
(40) Motekaitis, R. J., and Martell, A. E. (1991) Stabilities of the iron(III) chelates of 1,2-dimethyl-3-hydroxy-4-pyridinone and related ligands. *Inorg. Chim. Acta 183*, 71−80.
(41) Hider, R. C., and Liu, Z. D. (2003) Emerging understanding of the advantage of small molecules such as hydroxypyridinones in the treatment of iron overload. *Curr. Med. Chem. 10*, 1051−1064.
(42) Heinz, U., Hegetschweiler, K., Acklin, P., Faller, B., Lattmann, R., and Schnebli, H. P. (1999) 4-[3,5-bis(2-hydroxyphenyl)-1,2,4-triazol-1-yl]benzoic acid: a novel efficient and selective iron(III) complexing agent. *Angew. Chem., Int. Ed. 38*, 2568−2570.
(43) Rush, J. D., Maskos, Z., and Koppenol, W. H. (1990) Reactions of iron(II)nucleotide complexes with hydrogen peroxide. *FEBS Lett. 261*, 121−123.
(44) Rush, J. D., and Koppenol, W. H. (1988) Reactions of Fe^{II}nta and Fe^{III}edda with hydrogen peroxide. *J. Am. Chem. Soc. 110*, 4957−4963.
(45) Ogura, Y., and Yamazaki, I. (1983) Steady-state kinetics of the catalase reaction in the presence of cyanide. *J. Biochem. 94*, 403−408.
(46) Gebicka, L., Metodiewa, D., and Gebicki, J. L. (1989) Pulse radiolysis of catalase in solution. I. Reactions of O_2^- with catalase and its compound I. *Int. J. Radiat. Biol. 55*, 45−50.
(47) Lu, C., and Koppenol, W. H. (2005) Redox cycling of iron complexes of *N*-(dithiocarboxy)sarcosine and *N*-methyl-D-glucamine dithiocarbamate. *Free Radical Biol. Med. 39*, 1581−1590.

TX060101W